Volume 1 | Number 1 | Jan 2013 | Pages 1–100

Green Chemistry

Cutting-edge research for a greener sustainable future

www.rsc.org/greenchem

Stille couplings in water @RT

ROYAL SOCIETY OF CHEMISTRY

ROYAL SOCIETY OF CHEMISTRY

www.rsc.org/greenchem

Green Chemistry

COMMUNICATION

Highly Efficient, NiAu-catalyzed Hydrogenolysis of Lignin into Phenolic Chemicals

Jiaguang Zhang,[a] Hiroyuki Asakura,[b] Jeaphianne van Rijn, [a] Jun Yang,[c] Paul Duchesne,[d] Bin Zhang,[a] Xi Chen,[a] Peng Zhang,[d] Mark Saeys *[a] and Ning Yan*[a]

A highly efficient, stable NiAu catalyst that exhibits unprecedented low temperature activity in lignin hydrogenolysis was for the first time developed, leading to the formation of 14 wt% aromatic monomers from organosolv lignin at 170 ºC in pure water.

One of the central challenges for biomass utilization is the selective, catalytic hydrogenolysis of C–O bonds.[1-4] Hydrogenolysis will play a central role in future biorefineries, both for the production of value-added chemicals[5-7] and for the depolymerisation of raw biomass[8-10] such as lignin[11]. Indeed, the hydrogenolysis of lignin is an attractive route, among others[12-19], to transform the world's most abundant aromatic polymer into energy carriers and value-added chemicals. The first report of lignin depolymerisation dates back to 1938 and used high-loading copper-chromite catalysts and harsh reaction conditions.[20] Very few studies appeared in the following decades,[21] until recently a series of homogeneous and heterogeneous catalysts were reported for the hydrogenolysis of lignin and lignin model compounds.[22-30] Among these advances,

the selective C–O cleavage in lignin model compounds over Ni catalysts – a widely available and affordable metal – and under mild reaction conditions is particularly encouraging.[27-30] Nevertheless, several technological and scientific breakthroughs are required to make lignin hydrogenolysis industrially viable.[31] E.g., Ni-based catalysts show unsatisfactory activity for β-O-4 C–O bond hydrogenolysis (the most abundant linkage in lignin), due to both their limited activity (TOFs of 5-30 h^{-1})[27, 28] and their low dispersions (often below 5 %)[27]. Moreover, the relation between the electronic and geometric properties of the Ni catalyst and its hydrogenolysis activity and selectivity remain elusive, inhibiting the design of improved catalysts. Herein, we report the first development of a highly active and selective bimetallic NiAu catalyst, superior to reported heterogeneous Ni catalysts, for the hydrogenolysis of lignin model compounds and of organosolv lignin. The unusual structural features of the NiAu catalyst are identified, and the origin of the enhanced activity elucidated, providing guiding principles for catalyst design.

In a first step, the activity of 13 monometalic catalysts (Ru, Rh, Pd, Pt, Ir, Ag, Au, Cu, Fe, Co, Ni, Re and Sn) was screened for the hydrogenolysis of 2-phenoxy-1-phenethanol, a typical lignin model compound containing a β-O-4 linkage (Fig. 1a). Catalysts were prepared by aqueous phase reduction of equal amounts of metal salts with NaBH₄, employing poly(vinylpyrrolidinone) (PVP) as a stabilizing agent. The catalysts were tested immediately after preparation. Colloidal catalysts were selected as they might be more accessible to insoluble lignin than supported heterogeneous catalysts.[32] 15 products were identified (**1-15**, see Fig. 1a). Compounds **4-15** were identified by GC-MS analysis and confirmed using authentic samples. Compounds **1**, **2** and **3** are commercially unavailable and were identified by preparative HPLC and NMR

[a]*Department of Chemical and Biomolecular Engineering, National University of Singapore, 4 Engineering Drive 4, 117576, Singapore. Email: ning.yan@nus.edu.sg; saeys@nus.edu.sg*
[b]*Synchrotron Radiation Research Center, Nagoya University, Chikusa-ku, Nagoya 464-8603, Japan*
[c]*State Key Laboratory of Multiphase Complex Systems, Institute of Process Engineering, Chinese Academy of Sciences, Beijing, 100190, China*
[d]*Department of Chemistry and Institute for Research in Materials, Dalhousie University, Halifax, NS, B3H 4J3, Canada*

spectroscopy (see Supporting Information for NMR data). The products are categorized as monomers (**8-15**) and dimers (**1-7**). The yield of each dimer is defined as the molar ratio of this dimer to the starting material. The yield of each monomer is defined as 50 % of the molar ratio of this monomer to the starting material, considering one subtrate molecule can generate two monomeric products. As such, the total yield of **1-15** would reach 100% if the substrate conversion is complete. The yield of **8-15** provides an indication of the β-O-4 hydrogenolysis activity. Without metal catalysts no conversion of the substrate was observed. Among the 13 monometalic catalysts, Ni showed the highest selectivity towards monomers, although not the highest conversion, indicating a high β-O-4 hydrogenolysis selectivity. Note that hydrolysis products accounted for less than 0.5 % in all experiments. Detailed information on the conversion and the selectivity for each product can be found in the supporting information (Table S1).
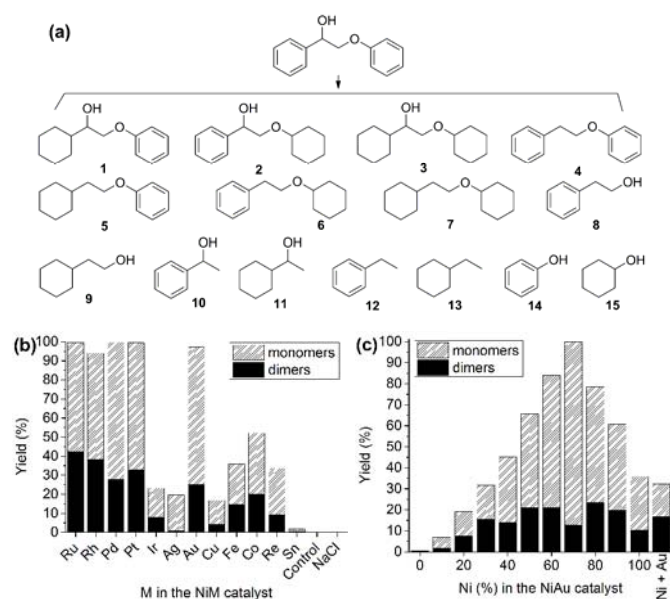
Fig. 1 (a) 15 products identified after 2-phenoxy-1-phenethanol hydrogenolysis; (b) Dimer and monomer yields for bimetallic NiM catalysts (Ni:M = 4:1). "Control" refers to a control experiment without metal catalyst but with 0.22 mmol NaBH₄ and 0.44 mmol PVP; whereas "NaCl" refers to a control experiment without metal catalyst but with 0.044 mmol NaCl, 0.22 mmol NaBH₄ and 0.44 mmol PVP. Reaction conditions: 0.22 mmol 2-phenoxy-1-phenethanol, 3 mL freshly prepared aqueous solution containing 0.022 mmol metal and 0.44 mmol PVP, 10 bar H₂, 130 °C, 2.5 h; (c) Dimer and monomer yields for bimetallic NiAu catalysts for different Ni:Au ratios. The bar on the right shows the performance of a physical mixture of monometallic Ni and Au catalysts (Ni:Au = 7:3). Reaction conditions: same as in (b) but shorter reaction time (1 h).

To increase the activity of the Ni catalysts, we evaluated the performance of 12 NiM bimetallic catalysts (Fig. 1b). The preparation of the bimetallic catalysts followed the procedure for the monometallic catalysts except that a second metal salt was added at a fixed M:Ni ratio (1:4). The introduction of 20 % Ru, Rh, Pd, Pt or Au had a significant promotional effect, leading to nearly quantitative conversion of 2-phenoxy-1-phenethanol after 2.5 hours. Surprisingly, the highest monomer yield of 72% was achieved over NiAu. Though monometallic Au catalysts are completely inactive for hydrogenolysis and the addition of Au to

Ni generally *reduces* catalyst activity, e.g., in carbon deposition[33, 34], in methane steam reforming[33, 34] and in dinitrobenzene hydrogenation[35-38], the addition of Au to Ni promoted hydrogenolysis of C–O bond in 2-phenoxy-1-phenethanol.

Next, the effect of the Ni:Au ratio on the activity was evaluated. The reaction time in this set of experiments was reduced from 2.5 to 1 hour. As expected, a volcano-type relationship between the metal ratio and the monomer yield was observed (Fig. 1c, Table S2), and an optimal Ni:Au ratio of 7:3 (denoted as Ni₇Au₃) was found. With the optimal Ni₇Au₃ catalyst 99% conversion of 2-phenoxy-1-phenethanol with an 87% monomer yield was obtained in just 1 hour under mild reaction conditions in water. With double amount of substrate, 87% conversion could still be achieved over Ni₇Au₃ in 3 hours (Table S4), suggesting the catalyst remains active. The metal ratio was confirmed by ICP-MS analysis (7.4:2.6). Note that a physical mixture of monometallic Ni and monometallic Au catalysts at the same ratio (7:3) was not effective for the reaction under the same conditions (monomer yield of 16%).
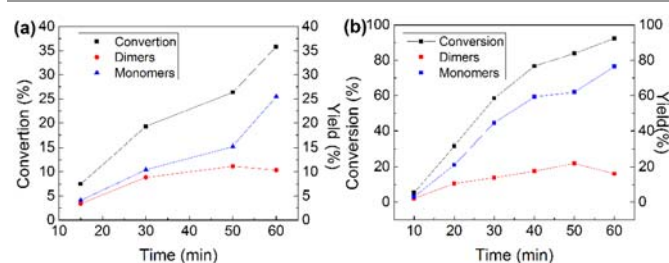
Fig. 2 Kinetics study on the hydrogenolysis of 2-phenoxy-1-phenethanol over (a) Ni catalysts and (b) Ni₇Au₃ catalysts. Reaction conditions: 2-phenoxy-1-phenethanol (0.22 mmol), freshly prepared Ni or Ni₇Au₃ catalysts water solution (3 mL, containing 0.022 mmol metal catalysts and 0.44 mmol PVP), 10 bar H₂, 130 °C.

The conversion of 2-phenoxy-1-phenethanol and the product distribution were studied as a function of time (Fig. 2, Table S4). For both Ni and Ni₇Au₃, the conversion increased with time without deactivation. The dimer yield increased during the first 50 min and then decreased, indicating dimers are reaction intermediates. At t = 0, the Ni₇Au₃ catalyst exhibits an activity three times higher than monometallic Ni. The number of accessible surface sites was determined by a CS₂ poisoning test.[39] This test assumes that CS₂ binds irreversibly to two surface Ni atoms.[40] The number of active sites is obtained by measuring the gradual decrease in activity as surface sites are titrated by CS₂ (Fig. S1). The CS₂ poisoning test gave dispersions of 10% for the monometallic Ni catalyst and 20% for the Ni₇Au₃ catalyst. With this dispersion, initial C–O hydrogenolysis TOFs of 30 h⁻¹ for the monometallic Ni catalyst and 47 h⁻¹ for the Ni₇Au₃ catalyst are obtained. The TOF for the monometallic Ni catalyst is comparable to the value of 26 h⁻¹ reported by He et al. under similar conditions[27]. The Ni₇Au₃ catalysts are hence more active due to increased activity per surface site and the increased dispersion. To our knowledge, the Ni₇Au₃ catalyst reported here displays the highest TOF for β-O-4 hydrogenolysis in model lignin compounds under these reaction conditions (see Table

S6). The *increase* in the hydrogenolysis rate per active Ni site by the introduction of an inert metal such as Au is moreover unprecedented.
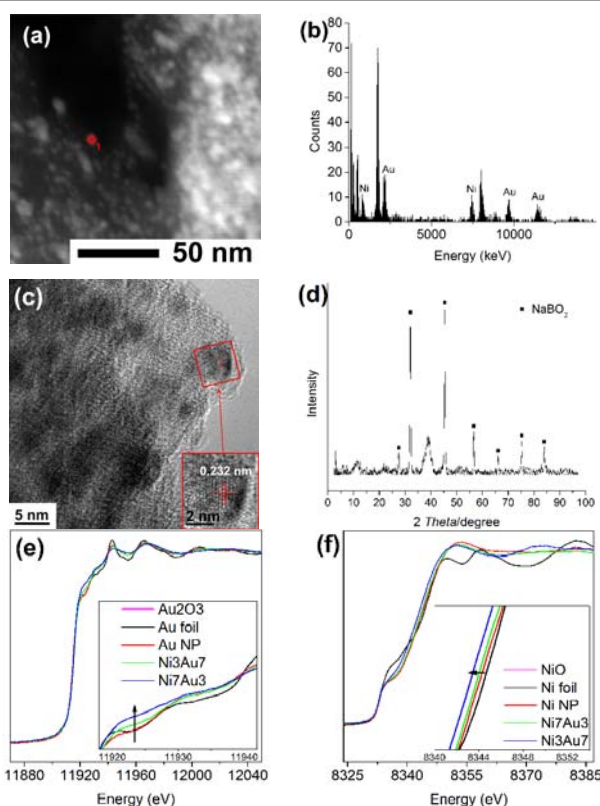
Fig. 3 (a) HAADF-STEM image of the Ni7Au3 catalyst; (b) Corresponding EDX spectrum for a selected particle (red circle in a)); (c) HRTEM image of Ni7Au3 catalyst; (d) XRD pattern of the Ni7Au3 catalyst; (e) Normalized XAS spectra at Au L$_{III}$ edge of Au, Ni3Au7 and Ni7Au3 catalysts. Spectrum of Au foil was included as a reference; (f) Normalized XAS spectra at Ni K edge of Ni, Ni3Au7 and Ni7Au3 catalysts. Spectrum of Ni foil was included as a reference.

Various characterization techniques were applied to probe the structural and electronic properties of the bimetallic Ni7Au3 catalyst. Transmission electron microscopy (TEM) shows spherical Ni3Au7 catalyst particles with a diameter of 4.1 ± 1.0 nm (Fig. S2c), compared to a diameter of 11.5 ± 3.5 nm for the monometallic Ni catalyst (Fig. S2a). These values agree with the dispersions measured by CS$_2$ poisoning. Particle specific energy dispersive X-ray (EDX) spectra of six randomly selected Ni7Au3 particles in high-angle annular dark-field scanning TEM (HAADF-STEM) images confirm that the particles are bimetallic (Fig. 3a-b, Fig. S3a-j). The high-resolution TEM (HRTEM) images also show a crystalline lattice with a lattice spacing of 0.232 nm (Fig. 3c), similar to the (111) plane of face-centred cubic (fcc) Au (0.235 nm).[41] The X-ray powder diffraction (XRD) pattern shows a broad peak at around $2\theta = 39°$ (Fig. 3d), corresponding to the (111) peak of Au (JCPDS file: 65-8601), in agreement with the HRTEM results. X-ray absorption near edge spectroscopy (XANES) demonstrated that both Ni and Au are metallic in the freshly prepared Ni7Au3 catalyst (Fig. 3e-f). Extended X-ray absorption fine structure (EXAFS) data show Au-Au, Ni-Ni and Au-Ni coordination

numbers (CN) of 8, 4 and 1-2, respectively (see Table S7-8, Fig. S4 for the fitting details). Using X-Ray photoelectron spectroscopy (XPS) a Ni:Au ratio of 3.8:1 was determined (Fig. 4, Table 1), suggesting a Ni-enriched shell. *In-situ* UV-vis spectra were recorded to follow the formation of the Ni, Au and Ni7Au3 catalysts at diluted conditions (Fig. S5). Monometallic Ni reduced very slowly whereas monometallic Au and bimetallic Ni7Au3 catalysts both formed immediately after adding NaBH4, suggesting Au catalyzed the reduction of Ni in the latter system.
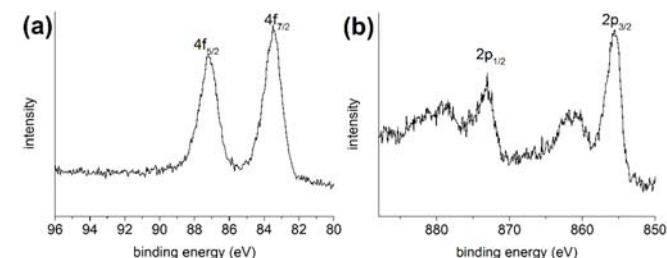
Fig. 4 XPS spectra of Ni7Au3 catalyst: (a) Au 4f region and (b) Ni 2p region.

Table 1. Surface concentration of major elements in Ni7Au3 catalyst.[a]

	C	N	O	Ni	Au	Ni:Au
Surface concentration	71%	10%	17%	1.3%	0.34%	3.8

[a] Determined by XPS peaks area corrected by corresponding relative sensitivity factors.
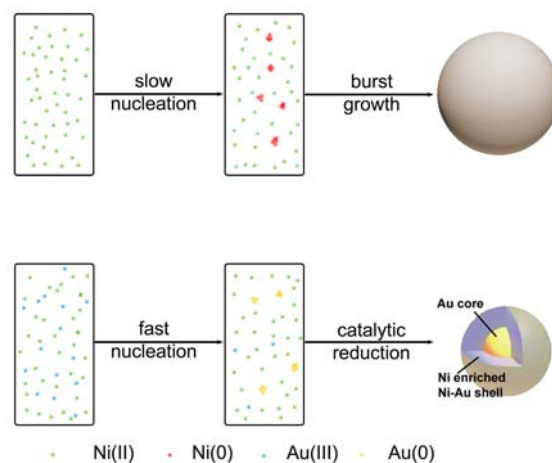
Scheme 1 The proposed two-stage formation process of Ni (top) and Ni7Au3 (bottom) catalysts.

In previous studies, a Ni core and Au-doped surface were generally proposed as the structure for NiAu catalysts.[33, 36, 42-44] However, the structure of the Ni7Au3 catalyst reported here appears to be radically different, and consists of a crystalline Au core and a Ni-enriched shell. This structure is based on the following observations: 1) EXAFS shows a high Au-Au CN and a low Ni-Ni CN, indicating that the majority of the Ni is located at the surface; 2) The Ni:Au ratio determined by XPS analysis (3.8:1) is higher than the stoichiometric ratio (2.3:1) and the ratio determined by ICP-MS (2.8:1), suggesting enrichment of Ni in the shell; and 3) the UV-vis experiments demonstrate that *in situ*

generated Au^0 species catalyze the reduction of Ni, suggesting that small Au clusters are formed first and act as nuclei for the growth of a Ni-rich shell. The nucleation-growth process of Ni (slow nucleation and rapid growth) and of Ni_7Au_3 (fast nucleation and catalytic growth) are illustrated in Scheme 1.
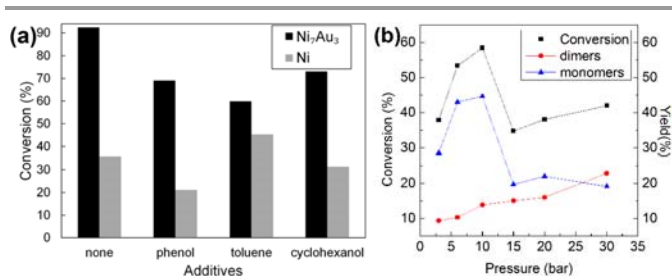
Fig. 5 (a) Influence of various additives on the reaction over Ni and Ni_7Au_3 catalysts; (b) Influence of H_2 pressure on the 2-phenoxy-1-phenethanol conversion and the product distribution over Ni_7Au_3 catalyst. Reaction conditions: 0.22 mmol 2-phenoxy-1-phenethanol, 3 mL freshly prepared aqueous solution containing 0.022 mmol metal and 0.44 mmol PVP, and for (a) 0.11 mmol additive, 10 bar H_2, 130 °C, 1h; for (b) 130 °C, 1h.

We first speculate that phenol desorption from the catalyst surface is rate-determining, and incorporation of Au into Ni decreases the desorption energy of aromatic products. To prove/disprove this assumption, the inhibition effect of two aromatic compounds (phenol and toluene) and cyclohexanol (as a control) were evaluated (Fig. 5a). In all cases, no significant inhibitions were observed in the case of pure Ni and NiAu catalysts, suggesting product desorption is not rate-determining. Ni and NiAu catalysts were also investigated with periodic Density Functional Theory calculations[45, 46] with the revised Perdew-Burke-Enzerhoff-Van der Waals functional (DFT-RPBE-VdW) as implemented in VASP[47]. Since the addition of CS_2 was found to gradually decrease the measured rate (Fig. S1), and the number of sites is consistent with the particle size, the system was based on terraces. A 3-layer, $p(4\times4)$ unit cell was used and a 3:1 Ni:Au ratio was used in the surface layer of the NiAu slab (Fig. S6). Phenol is found to prefer the bridge sites on Ni(111), in agreement with Della Site et al.[48] and adsorbs rather weakly with an adsorption energy of only 51 kJ/mol. Addition of Au caused the desorption of phenol during the calculations. The weak adsorption is consistent with the absence of product inhibition in the experiments (Fig. 5a).

To further analyze the origin of the unique promotional effect of Au, the hydrogenolysis rate as a function of the H_2 pressure was tested (Fig. 5b and Table S3). Between 3 and 10 bar, the rate over Ni_7Au_3 increased with H_2 pressure, whereas above 10 bar, the rate decreased with hydrogen pressure. The relationship between the reaction rate with H_2 pressure below 10 bar suggests that hydrogenation of a surface intermediate is a kinetically important step. We therefore studied the hydrogenation of adsorbed phenoxy (ArO*) intermediates and the effect of Au on this reaction step. Preliminary results show that on Ni(111), hydrogenation of phenoxy species has a surface reaction barrier of 161 kJ/mol (Fig. S6), suggesting this step is slow at 130 °C. Higher, more realistic surface coverages likely reduce this barrier.[49] Addition of Au destabilizes ArO* intermediates and

decreases the activation barrier by 21 kJ/mol, to 140 kJ/mol (Fig. S6), corresponding to a 500-fold increase in the rate coefficient at 130 °C. The addition of Au has a limited effect on the geometry of the transition state, and the O-H distance changes by less than 0.1 Å (Table S9).

The exceptional performance of the NiAu catalyst at a Ni:Au = 7:3 may be related to the unique electronic state of Ni in Ni_7Au_3. XANES spectra revealed the electronic modifications between Ni and Au (Fig. 3e-f). The white line intensity of Au increases with increasing Ni loading, pointing towards a decreased electron density of the Au atoms upon interaction with Ni. Concurrently, the absorption edge of Ni is shifted towards a lower energy as Au content increases. Combined it appears that Au acts as an electron donor in the NiAu catalyst, enabling neighbouring Ni atoms to be more electron enriched, which is in agreement with previous studies.[33] Probably, the electronic state of Ni is ideal for the lignin hydrogenolysis reaction at a Ni:Au ratio of 7:3.

Ni_7Au_3 shows high activity for the hydrogenolysis of a variety of lignin model compounds. Under the same reaction conditions, two other β-O-4 model compounds with methoxyl substitution and an α-O-4 model compound (1-benzyloxy-2-methoxybenzene) gave high monomer yields in 1 hour (Fig. S7, Table S10). Diphenyl ethers with a 4-O-5 linkage could also be converted efficiently to monomers (Table S11), although a longer reaction time was required.

Finally the performance of the bimetallic Ni_7Au_3 catalyst was evaluated for the hydrogenolysis of organosolv lignin under typical conditions (130 °C for 1 hour) and under harsher conditions (170 °C for 12 hours). Gel permeation chromatography (GPC) analysis shows the organosolv lignin has high MW, whereas the average MW decreases dramatically after hydrogenolylsis over Ni_7Au_3. The distribution for the products after reaction at 130 °C (**lignin130)** and at 170 °C (**lignin170)** are centered at 7.5 kDa and 1.3 kDa, respectively, the latter of which corresponds to a mixture of lignin monomer and oligomers, demonstrating complete depolymerization of organosolve lignin over Ni_7Au_3 (Fig. S8). The products were further analyzed by ^{13}C-NMR spectroscopy. Due to its polymeric nature, only a few broad peaks were observed for organosolv lignin (Fig. S9a). A series of new peaks appears in the product spectrum after reaction at 130 °C (lignin130, Fig. S9b). The chemical shifts at around 148 ppm, 120-140 ppm, 106 ppm, 50-60 ppm, 30 ppm correspond to phenoxy carbons, phenolic ring carbons, guaiacyl carbons, methoxy carbons, and methylene carbons,[50] respectively, indicating significant lignin depolymerization at 130 °C after 1 hour. On the other hand, the peak at 66.8 ppm corresponding to C-α in β-O-4 guaiacol was still observed, suggesting incomplete C–O hydrogenolysis. The number of peaks in the ^{13}C NMR spectrum decreases further after 12 hours at 170 °C (lignin170, Fig. S9c), but the peak intensity increases significantly indicating more fragmentated products. Notably the peak at 66.8 ppm reduced, which suggests significant β-O-4 breakage.

Most encouragingly, a series of monomers directly produced from lignin over Ni_7Au_3 catalyst were detected, identified, and

quantified by GC-MS and GC techniques. Reaction of lignin at 130 ºC for 1 h affords a monomer yield close to 2 wt% (Table 2). To our knowledge, direct production of monomeric aromatics from lignin under such mild reaction condition in water has never been reported before. Increase the reaction temperature to 170 ºC significantly increased the yield to 6 wt%, whereas merely 2 wt% monomer yield was achieved over pure Ni catalyst. An elongation of the reaction time to 12 h further increases the yield to ca. 14 wt%. No aromatic chemicals were observed when organosolve lignin reacts with $NaBH_4$ and PVP in water. Further adding NaCl into the system did not exhibit any improvement either. These experiments highlight that the monomeric aromatic compounds indeed originate from Ni_7Au_3 catalyzed hydrogenolysis.

Table 2 Organosolv lignin conversion over Ni_7Au_3 and Ni catalysts[a]

Catalyst	T (°C)	t (h)	Yield (wt%)		
Ni_7Au_3	130	1	0.5	1.0	0.3
Ni_7Au_3	170	1	1.4	3.8	0.6
Ni_7Au_3	170	12	3.2	9.3	1.7
Ni	170	1	0.5	1.6	0.1
$-^b$	170	1	0	0	0
$NaCl^c$	170	1	0	0	0

[a] Reaction conditions: 50 mg organosolv lignin, 3 ml freshly prepared aqueous solution containing 0.022 mmol metal and 0.44 mmol PVP, 10 bar H_2, reaction temperature and time can be found in table.

[b] Control experiment without metal catalyst but with 0.22 mmol $NaBH_4$ and 0.44 mmol PVP.

[c] Control experiment without metal catalyst but with 0.044 mmol NaCl, 0.22 mmol $NaBH_4$ and 0.44 mmol PVP.

Conclusions

In summary, an unexpectedly efficient and stable NiAu bimetallic catalyst was developed for lignin hydrogenolysis enabling 14 wt% of monomer yield under mild reaction conditions in pure water, which is three times more effective than pure Ni catalyst. The incorporation of Au significantly promotes the reduction of the Ni salt, resulting in the formation of small core-shell catalyst particles. More interestingly, the incorporation of Au in the Ni surface also increased the TOF, likely by destabilizing reaction intermediates and thereby increasing the hydrogenation activity of the catalyst. This study hence demonstrates the potential of enhancing the C–O hydrogenolysis activity by controllably manipulating the electronic and structural properties of Ni catalysts, providing guiding principles for future catalyst design for lignin valorization and beyond.

Acknowledgements

Notes and references

1. Y. Nakagawa and K. Tomishige, *Catal. Today*, 2012, **195**, 136-143.
2. A. Corma, S. Iborra and A. Velty, *Chem. Rev.*, 2007, **107**, 2411-2502.
3. A. M. Ruppert, K. Weinberg and R. Palkovits, *Angew. Chem. Int. Ed.*, 2012, **51**, 2564-2601.
4. H. Kobayashi, T. Komanoya, S. K. Guha, K. Hara and A. Fukuoka, *Appl. Catal., A*, 2011, **409–410**, 13-20.
5. M. Chia, Y. J. Pagán-Torres, D. Hibbitts, Q. Tan, H. N. Pham, A. K. Datye, M. Neurock, R. J. Davis and J. A. Dumesic, *J. Am. Chem. Soc.*, 2011, **133**, 12675-12689.
6. Y. Nakagawa, X. Ning, Y. Amada and K. Tomishige, *Appl. Catal., A*, 2012, **433–434**, 128-134.
7. M. Saidi, F. Samimi, D. Karimipourfard, T. Nimmanwudipong, B. C. Gates and M. R. Rahimpour, *Energy Environ. Sci.*, 2013.
8. Y. Liu, C. Luo and H. Liu, *Angew. Chem. Int. Ed.*, 2012, **51**, 3249-3253.
9. A. Fukuoka and P. L. Dhepe, *Angew. Chem. Int. Ed.*, 2006, **45**, 5161-5163.
10. N. Ji, T. Zhang, M. Zheng, A. Wang, H. Wang, X. Wang and J. G. Chen, *Angew. Chem. Int. Ed.*, 2008, **47**, 8510-8513.
11. J. Zakzeski, P. C. A. Bruijnincx, A. L. Jongerius and B. M. Weckhuysen, *Chem. Rev.*, 2010, **110**, 3552-3599.
12. M. R. Sturgeon, M. H. O'Brien, P. N. Ciesielski, R. Katahira, J. S. Kruger, S. C. Chmely, J. Hamlin, K. Lawrence, G. B. Hunsinger, T. D. Foust, R. M. Baldwin, M. J. Biddy and G. T. Beckham, *Green Chem.*, 2014.
13. J. Zhang, Y. Liu, S. Chiba and T.-P. Loh, *Chem. Commun.*, 2013, **49**, 11439-11441.
14. E. Feghali and T. Cantat, *Chem. Commun.*, 2013.
15. S. Son and F. D. Toste, *Angew. Chem. Int. Ed.*, 2010, **49**, 3791-3794.
16. A. Rahimi, A. Azarpira, H. Kim, J. Ralph and S. S. Stahl, *J. Am. Chem. Soc.*, 2013, 6415-6419.
17. M. Sturgeon, M. H. O'Brien, P. N. Ciesielski, R. Katahira, J. S. Kruger, S. C. Chmely, J. Hamlin, K. Lawrence, G. Hunsinger, T. D. Foust, R. Baldwin, M. J. Biddy and G. T. Beckham, *Green Chem.*, 2013.
18. Q. Song, F. Wang, J. Cai, Y. Wang, J. Zhang, W. Yu and J. Xu, *Energy Environ. Sci.*, 2013, **6**, 994-1007.
19. J. M. Nichols, L. M. Bishop, R. G. Bergman and J. A. Ellman, *J. Am. Chem. Soc.*, 2010, **132**, 12554-12555.
20. E. E. Harris and H. Adkins, *Pap. Trade J.*, 1938, **107**, 38-40.
21. J. M. Pepper and W. Steck, *Can. J. Chem.*, 1963, **41**, 2867-2875.
22. Y. Ye, Y. Zhang, J. Fan and J. Chang, *Bioresour. Technol.*, 2012, **118**, 648-651.
23. A. Wu, B. O. Patrick, E. Chung and B. R. James, *Dalton Trans.*, 2012, **41**, 11093-11106.
24. K. Barta, G. R. Warner, E. S. Beach and P. T. Anastas, *Green Chem.*, 2014.
25. Z. Strassberger, A. H. Alberts, M. J. Louwerse, S. Tanase and G. Rothenberg, *Green Chem.*, 2013, **15**, 768-774.
26. D. J. Rensel, S. Rouvimov, M. E. Gin and J. C. Hicks, *J. Catal.*, 2013, **305**, 256-263.
27. J. He, C. Zhao and J. A. Lercher, *J. Am. Chem. Soc.*, 2012, **134**, 20768-20775.
28. Q. Song, F. Wang and J. Xu, *Chem. Commun.*, 2012, **48**, 7019-7021.

29. A. G. Sergeev, J. D. Webb and J. F. Hartwig, *J. Am. Chem. Soc.*, 2012, **134**, 20226-20229.
30. A. G. Sergeev and J. F. Hartwig, *Science*, 2011, **332**, 439-443.
31. J. E. Holladay, J. F. White, J. J. Bozell and D. Johnson, *Top Value-Added Chemicals from Biomass Volume II—Results of Screening for Potential Candidates from Biorefinery Lignin* Northwest National Laboratory, Richland, WA., 2007.
32. A. Roucoux, J. Schulz and H. Patin, *Chem. Rev.*, 2002, **102**, 3757-3778.
33. Y.-H. Chin, D. L. King, H.-S. Roh, Y. Wang and S. M. Heald, *J. Catal.*, 2006, **244**, 153-162.
34. F. Besenbacher, I. Chorkendorff, B. S. Clausen, B. Hammer, A. M. Molenbroek, J. K. Nørskov and I. Stensgaard, *Science*, 1998, **279**, 1913-1915.
35. F. Cárdenas-Lizana, S. Gómez-Quero and M. Keane, *Catal. Lett.*, 2009, **127**, 25-32.
36. F. Cárdenas-Lizana, S. Gómez-Quero, C. J. Baddeley and M. A. Keane, *Appl. Catal., A*, 2010, **387**, 155-165.
37. F. Cárdenas-Lizana, S. Gómez-Quero, G. Jacobs, Y. Ji, B. H. Davis, L. Kiwi-Minsker and M. A. Keane, *J. Phys. Chem. C*, 2012, **116**, 11166-11180.
38. M. Dan, M. Mihet, A. Biris, P. Marginean, V. Almasan, G. Borodi, F. Watanabe, A. Biris and M. Lazar, *Reac. Kinet. Mech. Cat.*, 2012, **105**, 173-193.
39. L. S. Ott and R. G. Finke, *Coord. Chem. Rev.*, 2007, **251**, 1075-1100.
40. Z. Király, B. Veisz and Á. Mastalir, *Catal. Lett.*, 2004, **95**, 57-59.
41. Y. Yuan, N. Yan and P. J. Dyson, *Inorg. Chem.*, 2011, **50**, 11069-11074.
42. G. Yuan, C. Louis, L. Delannoy and M. A. Keane, *J. Catal.*, 2007, **247**, 256-268.
43. B. D. Chandler, C. G. Long, J. D. Gilbertson, C. J. Pursell, G. Vijayaraghavan and K. J. Stevenson, *J. Phys. Chem. C*, 2010, **114**, 11498-11508.
44. L. Deghedi, J.-M. Basset, G. Bergeret, J.-P. Candy, M. C. Valero, J.-A. Dalmon, A. De Mallmann, A.-C. Dubreuil and L. Fischer, *Stud. Surf. Sci. Catal.*, 2010, **175**, 617-620.
45. G. Kresse and D. Joubert, *Phy. Rev. B*, 1999, **59**, 1758-1775.
46. G. Kresse and J. Hafner, *Phy. Rev. B*, 1994, **49**, 14251-14269.
47. J. Klimeš, D. R. Bowler and A. Michaelides, *Phy. Rev. B*, 2011, **83**, 195131.
48. L. Delle Site, A. Alavi and C. F. Abrams, *Phy. Rev. B*, 2003, **67**, 193406.
49. M. Saeys, M.-F. Reyniers, J. W. Thybaut, M. Neurock and G. B. Marin, *J. Catal.*, 2005, **236**, 129-138.
50. Y. Zhao, N. Yan and M. W. Feng, *ACS Sustainable Chem. Eng.*, 2012, **1**, 91-101.